Study of the Behaviour of Containment Buildings of PWR-Type Reactors, Until Complete Failure in Case of LOCA

J. Brochard, L. Carretero
SOCOTEC Industrie,
3 av. du Centre, F-78182 St Quentin-en-Yvelines, France

A. Combescure
Commissariat à l'Energie Atomique, C.E.N. Saclay, D.E.M.T.,
B.P. No. 2, F-91190 Gif-sur-Yvette, France

R. Avet-Flancard
Commissariat à l'Energie Atomique,
Département de Sûreté Nucléaire,
B.P. No. 6, F-92260 Fontenay-aux-Roses, France

J. Dulac
Electricité de France, SEPTEN,
Tour EDF-GDF, F-92080 Paris la Défense Cedex 8, France

This paper presents the results of the nonlinear axisymetric analysis of the behaviour of containment buildings (PWR 900 MWe with metallic skin and PWR 1300 MWe without any skin), under LOCA pressure and temperature loadings. The evolutions of pressure and temperature from the accident are the following : increase of pressure 0.3 bar/hour and increase of temperature 2°C/hour.

Constitutive laws have been used for the different materials of the containment building.

For metals, plasticity models, with Von Misès yield criterion are available. For these models, the plasticity flow rule is defined by the Hill principle of normality, and isotropic strain hardening is assumed.

For concrete, the yield criterion is defined in the stress'es space by three surfaces. These yield surfaces represent three damage modes of concrete :

- crack tensile damage, with the criterion of the maximal principal stress
- shear damage, with the criterion of Drucker-Prager
- non linear variation of volume under hydrostatic compaction

Different damage modes can be activated together.

This thermomechanical study has been made with the Finite Element Method, and the CEASEMT system code has been used. The objectives of this study have been obtained :

- the pressure of the first fracture of concrete
- the pressure of trough fracture of concrete
- the ruin modes of the containment building

However, the spatial discretization of the structure used in this Finite Element analysis induces limitations to the quantitative evaluation of the fracture of concrete, because the informations about fractures are known only on discrete points. From this analysis, we are not able to show up phenomeneon like strain localizations.

These topics will be discussed in the paper.

1 - INTRODUCTION - DESCRIPTION OF STRUCTURES

The containment buildings of PWR type reactors are built with prestressed concrete. These are cylindrical structures with metallic skin for PWR 900 MWe, and without any skin for PWR 1300 MWe (Fig.1 and tables I-II).

The purpose of these studies are to determine the evolution of the concrete fissuration and the ruin modes of the buildings, loaded with pressure and temperature, over the nominal conditions.

In this paper, we mainly describe the PWR 900 MWe study, the method of calculation for the PWR 1300 MWe study being the same. However we shall give the main results for both studies.

2 - METHODS OF CALCULATION - MODELISATION OF THE STRUCTURE

In order to limit the calculation cost, without losing any information about the behaviour of the structure, we realise this study in two parts, with the appropriate boundary conditions (Fig.2).

We have modelised a length of one or two times $\sqrt{RT}$, R and t being respectively the radius and the thickness of the cylinder.

This non-linear, thermomechanic study has been solved by the finite element method, an axisymetric model (program INCA developed by CEA/DEMT).

The different parts of the structure have been modelised in the following way :

- 543 isoparametric massive elements for concrete (8-nodes quadrilaters and 6-nodes triangles)
- 175 2-nodes shell elements for the metallic skin
- 602 2-nodes special elements for prestress and vertical passive steels
- 304 1-node cable element for prestress and circonferential passive steels

Last at all, the rigidity of the ground has been simulated with springs.

3 - LOADS

The loads considered in this study are the following :

- basic loads
  . weight of the structure
  . vertical and horizontal prestress
  . weight of the internal structures

- accidental loads

. at the accident time

- temperature : 140°C on the steel skin and 20°C everywhere else
- internal pressure : 4 bars

. evolution with time

- temperature increase on the steel skin : 2°C/hour
- internal pressure increase : 0,3 bar/hour

In order to determine the temperature field at the nodes of the modelisation, we used the finite element method programm DELFINE (CEASEMT system) to solve the heat transient equation, with boundary conditions and physic properties depending on the temperature.

For this preliminary study, we realise a thermal model with 2207 4-nodes quadrilaters and 211 3-nodes triangles for concrete, 175 2-nodes shell elements for metallic skin. This model does not make the difference between steel and concrete. For this model, we consider the thermal conductivity value of concrete. The loaded concrete which has an insulation role has been considered. The temperatures obtained by programme DELFINE have been then interpolated on the nodes of the mechanical mesh.

4 - NUMERICAL METHOD OF NON LINEARITIES RESOLUTION IN PROGRAMM INCA

4.1 General scheme of the non linear resolution

In the finite element method, the equilibrium equation is :

$$B^T \sigma = F \tag{1}$$

where : B is the divergence operator acting on the stresses : σ

F load (nodal forces result)

When the convergence is reached the equilibrium equations are verified, the flow rules have been respected and the stresses are on the yield surfaces.

The methode based on the initial stress method is described in [1].

4.2 Concrete model : yield criteria and flow rules

The concrete model programmed in INCA considers non linear behaviours of concrete [2]. It takes into account three damage modes :

- crack damage
- shear damage
- hydrostatic compaction damage

The theory used in the development of this model is an extension of the plasticity with isotropic strain - hardening. For each damage mode, we use the three classic functions :

- yield criterion $F(\sigma_{ij}, H_k) = 0$ (2)

- flow rules $d\,\varepsilon_{ij}^{P} = d\lambda \dfrac{\partial \phi}{\partial \sigma_{ij}}$ (3)

- strain-hardening function H (t) $dH = f \left\{ d\varepsilon^P \right\}$ (4)

4.2.1 Crack damage

For crack damage, we choose a principal stress criterion :

$$\mathrm{Max} \left\{ \sigma_i \right\} = \sigma_t \quad i = 1, 2, 3 \tag{5}$$

σ_i i = 1, 2, 3 principal stresses of tensor σ_{ij}

σ_t maximum tensile stress

The yield surface associated with this criterion is a three faces pyramid in the principal stress space, whose vertex is $V(\sigma_t, \sigma_t, \sigma_t)$ and whose axis is parallel to the direction $\Delta : \sigma_1 = \sigma_2 = \sigma_3$ (Fig. 3).

The stress-strain curve associated with crack damage criterion is given on the principal stresses overflows the maximum tensile stress σ_t, this limit becomes 0 for that direction.

In the axisymetric case, this model considers two different fissuration modes : circonferential fissuration and in plane RZ fissuration.

Circonferential fissuration

The circonferential fissuration may be represented by a uniform distribution of radial cracks situated in vertical plans (Fig. 5).

In plane RZ fissuration

According to the orientation of the principal directions of stresses, the RZ fissuration may be represented by cuts in a slide less or more inclined on the horizontal of the structure (Fig. 6).

4.2.2. Shear damage

For the shear damage, we choose the Mohr-Coulomb's criterion.

$$|\tau_n| = c - \sigma_n \, t_g \varphi \tag{6}$$

. τ_n shear stress
. σ_n normal stress

. c cohesion

. φ angle of internal friction

The yield surface associated with the Mohr-Coulomb's criterion is an irregular hexagonal pyramid in the principal stress space, whose axis is parallel to the direction $\sigma_1 = \sigma_2 = \sigma_3$ and whose vertex is V (v,v,v), with $v = c \cot g \varphi$ (Fig.7).

Two triaxial compression stress-strain curves corresponding to two different levels of lateral pressure $\sigma_3{}^i$ are shown on the Fig.8.

4.2.3. Hydrostatic compaction damage

The stress-strain curve is given on Fig.9.

5 - RESULTS

The results, at different times of the non linear evolution, are presented through three points of view :

- deformation of structure
- damage of concrete
- plastification of metals

5.1 Deformation of structure

The evolution of the deformation of the structures, drawned with program ESPACE (CEASEMT system), are shown on Figs. 10-12 for PWR 900 MWe, and on Figs. 11-13 for PWR 1300 MWe.

The deformed shapes at last converged time show that the structure will ruin in the cylindrical part and in the dome for both type of reactor.

5.2 Damage of concrete

For our study, only the tensile and shear damages have been studied.

The program ESPACE draws three types of figures to represent the cracks in the concrete (Figs. 14-15-16).

These figures show the propagation direction of fissures and allow us to know the time of first fissuration and through fracture of concrete. The determination of the through fracture is a difficult task : the "type 2" figures have been developed to find the through fracture.

5.3 Plastification of metals

The structure ruins first by a loss of rigidity due to the cracking of the concrete so that the steels sustain the structure. The complete failure of the structure is obtained when the prestressed steels go into plasticity. This corresponds to :

(1) PWR 900 MWe

27-28 hours : rupture of the prestressed steels at the same time in the dome and in the cylinder.

(2) PWR 1300 MWe

14 hours : rupture of the prestressed steels in the dome.

5.4 Damage modes and ruin - modes of the containment building

At rest, the prestressed structure is subjected to its weight and the structures' weight.

At the first time of accident, the temperature gradient in the concrete thickness is very important. On the internal boundary, a little thickness of concrete is very hot, and at the same time the external part of concrete is still cold. The hot concrete dilatation produces a high force towards the exterior, causing the fissuration of still cold concrete on a thickness of 75 cm. at the time of half an hour. The little thickness of still hot concrete remains in compression. After this thermal break phase, and when the temperature field penetrates through the concrete, the influence of pressure becomes more and more important. The fissuration propagation is slower. Through fracture happens much later. When the concrete is cracked, it does not give any more stiffness to the structure, and than only the prestressed cables and passive steels support all the loads. The internal pressure governs the ruin of the containment building which will be initiated by the rupture of the prestressed cables.

6 - CONCLUSION

These studies give, with a good precision, the time of complete ruin of structures which happens a long time after through fracture of concrete, by break of prestressed cables. On the other hand, one of the main limits of these calculations is the indetermation on time of through fracture of concrete. In fact, the calculation by the finite element method takes in account a discretization of the structure, so that it is impossible to have a good precision on the first time when we can find a through crack. Another limitation is the fact that the concrete model considers a uniform distribution of cracks and does not at all take into account the fissures concentrations. More informations are given in [3] [4].

REFERENCES

[1] HOFFMANN, A., JEANPIERRE, F., CHARRAS, T., COMBESCURE, A., "Système CEASEMT. Apercus théoriques sur les programmes. Eléments - Dynamique - Non linéarités géométriques - Flambage - Plasticité", Rapport EMT/78/35. (Avril 1978).

[2] CARRETERO, L., COMBESCURE, A., "Un modèle non linéaire de comportement du béton", Rapport EMT/SMTS/79/34. (Novembre, 1979).

[3] CARRETERO, L., AOUSTIN, J., COMBESCURE, A., HOFFMANN, A., "Etude du comportement thermomécanique des enceintes de confinement des PWR 1300 MWe au delà des conditions de dimensionnement", Rapport EMT/SMTS/BAMS/80/29.

[4] CARRETERO, L., AOUSTIN, J., COMBESCURE, A., HOFFMANN, A., "Etude complète du comportement des enceintes de confinement des PWR 900 MWe au-delà des conditions de dimensionnement", Rapport EMT/SMTS/BAMS/80/30.

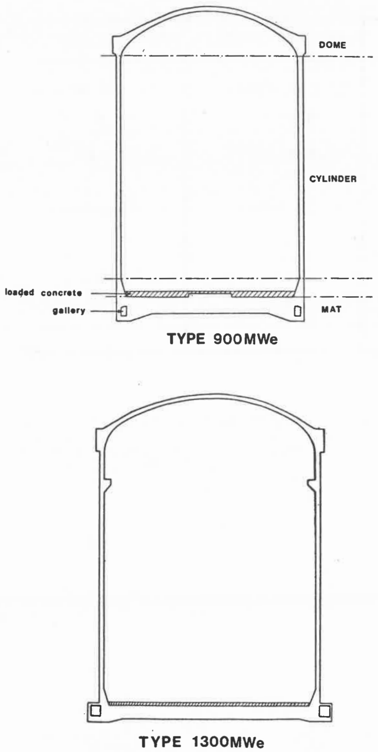

Fig. 1 : Cross sections of containment buildings

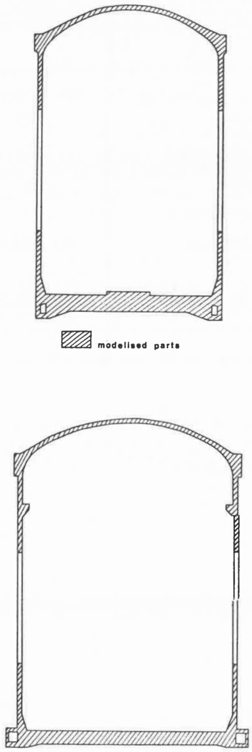

Fig. 2 : Modelisation of the structures

TABLE I : Main dimensions of containment buildings

	Type 900 MWe	Type 1300 MWe
Total height	66.18 m	70.60 m
Cylinder thickness	0.90 m	0.90 m
Outer diameter	19.40 m	23.40 m
Loaded concrete thickness	1.0 m	0.60 m
Mat thickness	3.50 m	3.00 m

TABLE II : Properties of materials

	CONCRETE	STEELS		
		Metallic skin	passive steels	prestressed steels
Young's modulus	4000 hbars	20 000 hbars	20 000 hbars	19 500 hbars
Poisson's ratio	0.2	0.3	0.3	0.3
Thermal expansion coefficient	1×10^{-5}	$1{,}2 \times 10^{-5}$	$1{,}2 \times 10^{-5}$	$1{,}2 \times 10^{-5}$
Yield stress		30 hbars	39 hbars	150 hbars
Maximum tensile stress	40 hbars			
Maximum compression stress	500 hbars			

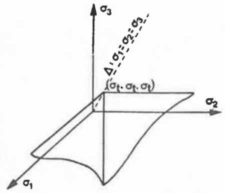

Fig. 3 : Crack damage : yield surface

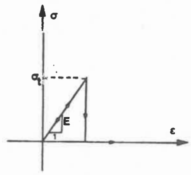

Fig. 4 : Crack damage : stress-strain curve

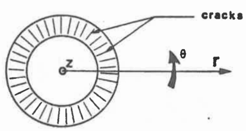

Fig. 5 : Crack damage :
circonferential fissuration

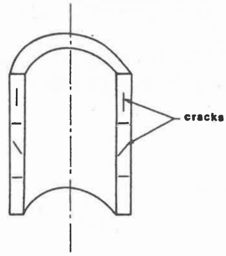

Fig. 6 : Crack damage :
in plane RZ fissuration

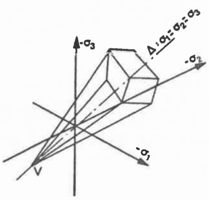

Fig. 7 : Shear damage : yield surface

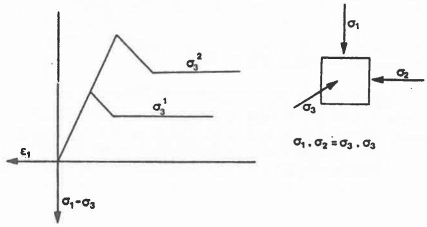

Fig. 8 : Shear damage : Stress-strain curves

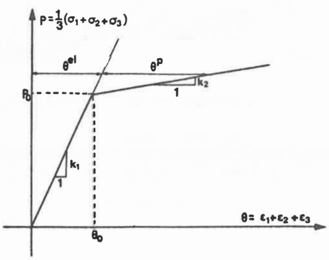

Fig. 9 : Hydrostatic compaction damage :
stress-strain curve

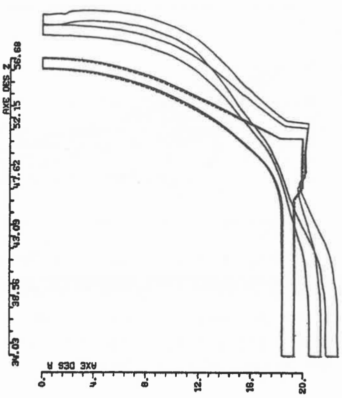

Fig. 10 : PWR 900 MWe - deformed shapes at times
0,18 and 27 hours

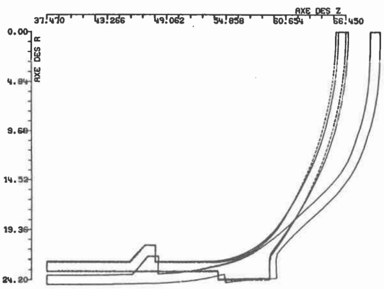

Fig. 11 : PWR 1300 MWe - deformed shapes at times 0,9 and 14h15mm

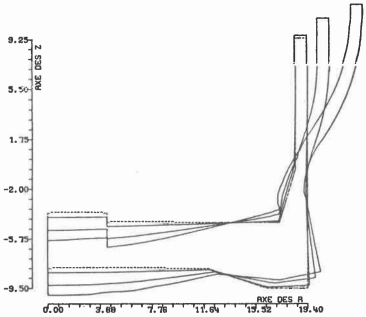

Fig. 12 : PWR 900 MWe - deformed shapes at times 0,14 and 28 hours

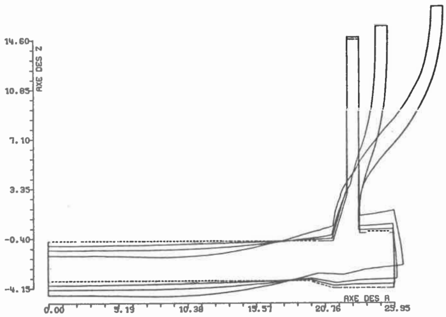

Fig. 13 : PWR 1300 MWe - deformed shapes at times 0,12 and 28 hours

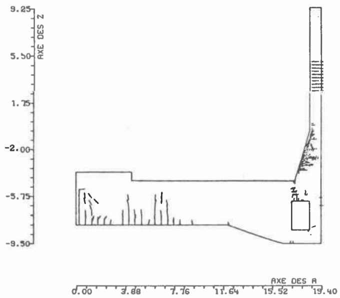

Fig. 14 : Type 1 : (for RZ fissuration) lines showing the direction of cracks at nodes

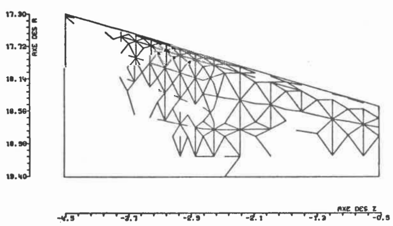

Fig. 15 : Type 2 : (for RZ and θ fissuration) lines joining the nodes, where there are cracks, with the centre of the corresponding element.

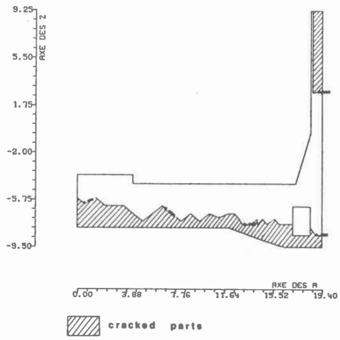

Fig. 16 : Type 3 : (for θ fissuration) isocurve $\sigma_{\theta} = 0$